Superexchange and Spin−Orbit Coupling in Chlorine-Bridged Binuclear Cobalt(II) Complexes

K. Fink,* C. Wang, and V. Staemmler

Lehrstuhl für Theoretische Chemie, Ruhr-Universität Bochum, D-44780 Bochum, Germany

Received March 12, 1999

Quantum chemical ab initio calculations are performed for the magnetic exchange coupling in binuclear chlorine-bridged Co(II) complexes of the form $L_3CoCl_3CoL_3$. In order to simplify the calculations, the terminal ligands are replaced with He-type model ligands L. The calculations are carried out at the restricted open-shell Hartree−Fock (ROHF), complete active space SCF (CASSCF), and valence configuration interaction (VCI) levels, with inclusion of spin−orbit coupling and external magnetic fields. The 12-fold degenerate $^4T_{1g}$ ground state of the Co^{2+} cation in a perfect octahedral ligand field is split by the trigonal distortion in the complex and by spin−orbit coupling. Both effects have the same order of magnitude, 200−500 cm^{-1}. The ground state of either cation is a Kramers doublet, $E_{1/2}$, separated by about 300 cm^{-1} from the lowest excited states. The coupling of the two $E_{1/2}$ ground states through the chlorine bridges is antiferromagnetic; the binuclear complex has a nondegenerate A_2'' ground state, followed by a nondegenerate first excited A_1' state 15 cm^{-1} above the ground state and a 2-fold degenerate second excited E″ state at 57 cm^{-1}. The next states are about 300 cm^{-1} higher in energy. From these energy levels the magnetic susceptibility χ is calculated by means of a Boltzmann average. χ shows a substantial anisotropy: $\chi_{||}$ is rather large because of a first-order Zeeman splitting of the E″ state in a magnetic field parallel to the molecular axis, while $\chi_\perp$ is small since it is only caused by second-order Zeeman effects. The calculated temperature dependence of χ agrees fairly well with experimental data; however, a phenomenological Heisenberg−Dirac−van Vleck Hamiltonian cannot be used to describe the measured susceptibility data.

I. Introduction

The magnetic properties of most bi- and polynuclear transition metal complexes, in particular the temperature dependence of the magnetic susceptibility $\chi(T)$, can be described fairly well by means of two parameters.[1] One of them is the *g*-factor, which determines the Zeeman splitting of degenerate electronic levels in an external magnetic field *B*,

$$E = -g\beta BM \tag{1}$$

where *M* is the magnetic quantum number of the state involved and

$$\beta = \frac{e\hbar}{2mc} \tag{2}$$

is Bohr's magneton. The second parameter is the exchange integral *J* in the Heisenberg Hamiltonian,

$$\hat{H} = -2J\vec{S}_1\cdot\vec{S}_2 \tag{3}$$

which describes the direct or indirect coupling between the spins (or total angular momenta) $\vec{S}_1$ and $\vec{S}_2$ of two transition metal cations in the complex. In the notation used in eq 3, negative values for *J* indicate antiferromagnetic and positive values ferromagnetic coupling.

In most cases, the electronic ground states of the cations in the transition metal complex are spatially nondegenerate. For instance, the Cr(III) or Ni(II) ions in octahedral coordination have $^4A_{2g}$ and $^3A_{2g}$ ground states, respectively. In such cases, the orbital angular momenta are totally quenched and eqs 1 and 3 are valid in their "spin only" form, with $g = g_e = 2.0023$ and $M = M_S$.

There are, however, more complicated cases, in which the ground states of the transition metal cations possess both space and spin degeneracy, e.g., Ti(III) ($^2T_{2g}$) or Co(II) ($^4T_{1g}$) in octahedral coordination or Ni(II) ($^3T_2$) in tetrahedral coordination. In these cases, the space−spin degeneracy is partly or fully removed by spin−orbit interaction. The spin−orbit coupling constant amounts to 100−500 cm^{-1} in the first transition metal series[2] and is therefore comparable with kT (∼200 cm^{-1} at room temperature) and with the exchange integral *J*, but much larger than the Zeeman splitting, even in strong laboratory fields of about 10 T. It is therefore compulsory to account for spin−orbit coupling (SOC) effects both in the analysis of experimental data and in ab initio calculations of magnetic properties of complexes or crystals containing such ions. In experimental investigations, SOC is generally accounted for by introducing a "zero field splitting" term

$$H_{ZFS} = \vec{S}\cdot D\cdot\vec{S} \tag{4}$$

in the phenomenological Hamiltonian,[1] but such a term also takes care of distortions of the octahedral geometry.

In a series of recent papers[3−7] we have performed quantum chemical ab initio calculations for the magnetic exchange

(1) Kahn, O. *Molecular magnetism;* VCH Publishers: New York, Weinheim, 1993.

(2) Moore, C. E. *Atomic energy levels;* Circular 467; Nat. Stand. Ref. Data Ser., Nat. Bur. Stand.: Washington, 1971.
(3) Fink, K.; Fink, R.; Staemmler, V. *Inorg. Chem.* **1994**, *33*, 6219.
(4) Wang, C.; Fink, K.; Staemmler, V. *Chem. Phys.* **1995**, *192*, 25.
(5) Wang, C.; Fink, K.; Staemmler, V. *Chem. Phys.* **1995**, *201*, 87.
(6) Fink, K.; Wang, C.; Staemmler, V. *Int. J. Quantum Chem.* **1997**, *65*, 633.
(7) Staemmler, V.; Wang, C.; Fink, K. To be published.

10.1021/ic990280n CCC: $18.00
Published on Web 08/07/1999

coupling in several oxygen- and sulfur-bridged binuclear transition metal complexes: linear oxygen-bridged $Ti^{III}OTi^{III}$, $V^{III}OV^{III}$, and $Cr^{III}OCr^{III}$ complexes,[3] geometry dependence of J in $Cr^{III}OCr^{III}$ [4] and in $Ni^{II}ONi^{II}$ as well as in $Ni^{II}O_2Ni^{II}$ complexes,[5] $Ni^{II}S_nNi^{II}$ complexes with $n = 1, 2, 3$,[6] and finally also bulk NiO and Cr_2O_3.[7] In all of these systems, SOC was not included, because the metal ions involved have spatially nondegenerate ground states or, as for the Ti(III) and V(III) complexes,[3] SOC is small compared to the exchange coupling.

In the present study we extend our theoretical treatment to binuclear Co(II) complexes, with the Co^{2+} ions in a distorted octahedral environment. In order to understand the magnetic properties and in particular the low-temperature dependence of the magnetic susceptibility $\chi(T)$ of such complexes, we will treat geometrical distortions, exchange splittings, and SOC simultaneously in an extended valence configuration interaction (CI) scheme. Furthermore, in order to achieve a direct comparison with experimental data, we will explicitly calculate $\chi(T)$ instead of just extracting parameters such as g or J from our CI calculations and comparing them with the corresponding parameters derived from experimental $\chi(T)$ curves.

There have been only very few bridged binuclear Co(II) complexes reported in the literature.[8−12] In all of them, the Co(II) ions are found to be weakly antiferromagnetically coupled. Numerical values for g and J have been determined by De Munno et al.[10] for several $[Co(bipym)Co]^{4+}$ complexes (bipym = 2,2′-bipyrimidine) and by Nühlen[11,12] for $[CoCl_3Co]^+$. A rather large isotropic value for g, $g = 2.86$, and a small antiferromagnetic exchange integral J of about -13 cm^{-1} were found in the latter study; the large deviation of the g-factor from the spin-only value $g_e = 2.0023$ is particularly remarkable. De Munno et al.[10] obtained reasonable fits to their experimental susceptibility data with $J \sim -5$ cm^{-1} and strongly anisotropic g-factors, $g_{\parallel} \sim 8.5$ and $g_{\perp} \sim 2.0$.

For an excellent discussion of the magnetic properties of transition metal complexes we refer to the book by O. Kahn.[1] It also contains a semiempirical analysis of the influence of SOC on the exchange interaction in $Cl_3TiCl_3TiCl_3$, which is related to the present ab initio work. A theoretical analysis of the effect of SOC on the lowest states of Co(II) clusters has been given by Lines,[13] but this discussion is also based on empirical parameters. To our knowledge, no ab initio treatment of SOC effects and g-factors in bridged binuclear Co(II) complexes has been published so far. The critical analysis of the exchange interaction in $Ti_2Cl_9^{3-}$ by Ceulemans et al.[14] does not contain SOC effects.

The present paper is organized as follows: Section II contains the description of our numerical method, in particular how SOC and external magnetic fields are included in the configuration interaction treatment. In section III several mononuclear Co(II) complexes are studied in order to analyze the effects of geometrical distortions and SOC on the electronic energy levels of a single Co^{2+} ion and to scale the spin−orbit coupling constant. Finally, section IV contains the results for the energy levels of the binuclear $CoCl_3Co$ complex, with inclusion of SOC and magnetic fields; from these energy levels are calculated exchange splittings, g-factors, and the temperature dependence of the magnetic susceptibility.

II. Method of Calculation

The isolated Co^{2+} ion has the electronic configuration $3d^7$ with an ^4F ground state ($S = 3/2$, $L = 3$). The next states are ^4P at 15 202 cm^{-1}, ^2G at 16 978 cm^{-1}, and so forth;[2,15] these values are the excitation energies of the lowest term in a given multiplet. The $3d^7$ configuration consists of 120 states, if each spin and angular momentum component is counted separately. In other words, it needs 120 different configuration state functions or Slater determinants to describe all states belonging to the $3d^7$ manifold. The ^4F ground state itself is 28-fold degenerate, as long as SOC is not accounted for.

In the reduced symmetry of an octahedral ligand field, the ^4F ground state of the free Co^{2+} ion is split into a $^4T_{1g}$ ground state (12-fold degenerate), a first excited $^4T_{2g}$ state (also 12-fold degenerate) at about 8000 cm^{-1}, and a second excited $^4A_{2g}$ state (4-fold degenerate) at about 14 000 cm^{-1}.[16] In this second excited state, the orbital angular momentum is completely quenched, but the spin degeneracy is preserved. If the octahedral symmetry at the Co^{2+} ion is further lowered by a trigonal distortion to C_{3v}, the $^4T_{1g}$ ground state is split into a $^4A_2$ and a ^4E component.

In the binuclear $Co^{II}Cl_3Co^{II}$ complex, the 12 components of the $^4T_{1g}$ ground states at either Co^{2+} ion give rise to 144 low-lying "pair" states, nine septets, quintets, triplets, and singlets, which are split by the trigonal distortion, spin−orbit coupling, and exchange interaction. The next states follow about 8000 cm^{-1} higher in energy.

A. Calculations without Spin−Orbit Coupling. The ab initio calculations for the $L_3CoCl_3CoL_3$ complex were performed in essentially the same way as in our previous studies[3−7] by means of the Bochum suite of programs[17−20] consisting of restricted open-shell Hartree−Fock (ROHF of SCF), complete active space SCF (CASSCF), configuration interaction (CI), and multiconfiguration coupled electron pair approach (MC-CEPA) programs. The following steps were carried out:

(a) The rather bulky terminal ligands, which are necessary in the experimental work to stabilize the complexes, are replaced by He-like model ligands L, constructed in the same way as for the $L_5Cr^{III}OCr^{III}L_5$ complex.[3] In order to generate the correct ligand field strength and to make the whole complex charge neutral, the Co−L distance was set to 1.683 Å and the charge of the model ligands to 1.83.

(b) A CASSCF calculation, averaged over all nine low-lying septet states, was performed for determining the MOs of the binuclear complex. The active space consisted of the 10 3d-AOs at the two metal cations, with a total occupation of 14 electrons. The 3p-AOs of the bridging Cl^- anions as well as the orbitals at the model ligands were kept in the inactive space.

(c) A clear-cut distinction between covalent ("neutral") and charge transfer ("ionic") configurations as well as between the direct ferromagnetic and the superexchange-type antiferromag-

(8) Couldwell, C.; Husain, J. *Acta Crystallogr. B* **1978**, *34*, 2444.
(9) Chaudhuri, P.; Querbach, J.; Wieghardt, K.; Nuber, B.; Weiss, J. *J. Chem. Soc., Dalton Trans.* **1990**, 271.
(10) De Munno, G.; Julve, M.; Lloret, F.; Faus, J.; Caneschi, A. *J. Chem. Soc., Dalton Trans.* **1994**, 1175.
(11) Nühlen, D. Masters Thesis, Ruhr-Universität Bochum, 1994.
(12) Bossek, U.; Nühlen, D.; Bill, E.; Glaser, T.; Krebs, C.; Weyhermüller, T.; Wieghardt, K.; Lengen, M.; Trautwein A. X. *Inorg. Chem.* **1997**, *36*, 2834.
(13) Lines, M. E. *J. Chem. Phys.* **1971**, *55*, 2977.
(14) Ceulemans, A.; Heylen, G. A.; Chibotaru, L. F.; Maes, T. L.; Pierlot, K.; Ribbing, C.; Vanquickenborne, L. G. *Inorg. Chim. Acta* **1996**, *251*, 15.
(15) Sugar, J.; Corliss, C. *J. Phys. Chem. Ref. Data* **1985**, *14*, Suppl. 2, 529.
(16) Banci, L.; Bencini, A.; Benelli, C.; Gatteschi, D.; Zanchini, C. *Struct. Bonding* **1982**, *52*, 37.
(17) Staemmler, V. *Theor. Chim. Acta* **1977**, *45*, 89.
(18) Wasilewski, J. *Int. J. Quantum Chem.* **1989**, *36*, 503.
(19) Meier, U.; Staemmler, V. *Theor. Chim. Acta* **1989**, *76*, 95.
(20) Fink, R.; Staemmler, V. *Theor. Chim. Acta* **1993**, *87*, 129.

netic contributions to the exchange integral J can only be made if localized "magnetic" orbitals are used instead of the delocalized canonical MOs. We applied the Boys criterium[21] for localizing the active orbitals. Of course, the CASSCF results as well as the full valence CI results (see below) are independent of whether localized or canonical orbitals are employed.

(d) Starting from the CASSCF orbitals a full valence configuration interaction (VCI) calculation was performed to determine the energies of the low-lying quintet, triplet, and singlet states in addition to those of the septets. Since all of these states are derived from the same $^4T_{1g}$ states of the two metal ions and are very close in energy, the CASSCF orbitals determined for the high-multiplicity states yield a reasonable description also for the states with lower spins. A further CASSCF optimization of the low-spin states does not lead to noticeable changes in the relative energies or in the exchange splittings.

(e) Since the superexchange contribution to J is largely underestimated in CASSCF or VCI calculations,[3-7] it is necessary to include dynamic correlation effects. Because of the large number of configurations in the CASSCF reference wave functions, a MC-CEPA treament for the present systems would be quite time-consuming. Therefore, we used our "modified VCI scheme" [7] to estimate the influence of correlation and relaxation effects on J.

The test calculations for the mononuclear complexes and the CoO clusters as presented in section III were performed in the same way as for the binuclear complex.

Basis sets of contracted Gaussians were used throughout the paper, for the conventional CI calculations as well as for the treatment of SOC and Zeeman splitting. The basis sets for the constituent atoms had essentially TZP quality (triple-ζ plus one set of polarization functions). For Co^{2+} we used the Wachters[22] 15s9p5d set contracted to 10s6p4d and augmented by one f set ($\eta_f = 1.8$). The Cl^- anions were described by a slightly modified 13s9p Huzinaga set[23] contracted to 9s6p and augmented by one d set ($\eta_d = 0.26$). For the He-like ligands we optimized a 7s basis set with exponents 30.2, 9.8, 3.5, 1.4, 0.55, 0.17, 0.05 and contracted it to 3s. Finally, in the cluster calculations for CoO the O^{2-} anions were described by a Huzinaga 9s5p set, contracted to 6s3p and augmented by a set of semidiffuse s and p functions ($\eta_s = \eta_p = 0.1$) to account for the large spatial extent of the O^{2-} anions. Some of the calculations were also performed with slightly modified basis sets, e.g., without diffuse s functions at Co^{2+} or with different contraction of the d functions. But since neither the superexchange splitting nor the SOC is sensitive to such modifications of the basis, we will not refer to them in the following.

The geometry of the $CoCl_3Co$ unit was fixed to the X-ray structure as determined by Nühlen[11] $R(Co-Cl) = 2.46$ Å, CoClCo angle $\alpha = 76.6°$. The whole $L_3CoCl_3CoL_3$ complex has D_{3h} symmetry.

B. Spin−Orbit Coupling and Zeeman Splitting. Both spin−orbit coupling and Zeeman splitting were included at the VCI level by explicitly calculating the matrix elements of the corresponding microscopic Hamiltonians. For this purpose the CASSCF orbitals were used without further modification. The VCI calculations with inclusion of SOC and a magnetic field B can be performed in two different N-electron basis sets:

(i) Determinantal Basis. Let $|I\rangle$ denote the Slater determinants (or the configuration state functions) that span the full active space. The Hamiltonian matrix with inclusion of SOC and magnetic field

$$\langle I|H_0 + \xi H_{SOC} + H_Z|J\rangle \tag{5}$$

is calculated in the basis of the Slater determinants and is then diagonalized. H_0 denotes the nonrelativistic Hamilton operator,

$$H_{SOC} = \sum_\alpha \sum_i \frac{Z_\alpha}{(R_\alpha - r_i)^3} \vec{l}_i \cdot \vec{s}_i \tag{6}$$

is the microscopic one-electron spin−orbit interaction (for the parameter ξ see below) and

$$H_Z = \sum_i \beta(\vec{l}_i + g_e \vec{s}_i)\cdot\vec{B} \tag{7}$$

is the Zeeman interaction with the external magnetic field $\vec{B}$, with $\vec{l}_i$ and $\vec{s}_i$ being the orbital angular momentum and spin operators for the ith electron and $g_e = 2.0023$ the spin-only g-factor.

(ii) Basis of the VCI Eigenfunctions. Alternatively, one can first determine the VCI eigenfunctions $|iSM_S\rangle$ of H_0 without SOC and Zeeman terms. They are also eigenfunctions of S^2 and S_z and linear combinations of the Slater determinants $|I\rangle$,

$$|iSM_S\rangle = \sum_I c_{iSM,I}|I\rangle \tag{8}$$

In a second step the matrix of the SOC and Zeeman splitting

$$\langle iSM_S|\xi H_{SOC} + H_Z|i'S'M_S'\rangle \tag{9}$$

is evaluated in the basis of the eigenfunctions $|iSM_S\rangle$ and diagonalized.

Of course, the two schemes yield identical results as long as the full space is employed, spanned by either $|I\rangle$ or $|iSM_S\rangle$. However, the use of the VCI eigenfunctions offers the possibility of calculating SOC and Zeeman effects only in a certain subspace, e.g., that of the low-lying states which are involved in the exchange coupling.

It should be noted that both H_{SOC} and H_Z couple states with different values of M_S and S. Therefore, the VCI with inclusion of H_{SOC} and H_Z cannot be performed for each value of M_S separately, but needs the full basis of all determinants, with M_S ranging from $+3$ to -3 in the present case of $Co^{II}Cl_3Co^{II}$.

In the present study we have only included the one-electron part of the SOC and omitted the very time-consuming two-electron part, i.e., the spin−other orbit coupling (SOOC). Since the latter generally reduces the SOC splittings by 30−50% without causing any qualitative changes,[24] we have simulated its effect by simply scaling our SOC results by a factor ξ, as already introduced in eqs 5 and 9. The scaling factor was determined by comparing the unscaled SOC splittings for the (^4F) ground state of the isolated Co^{2+} ion with experimental data.[2]

The Zeeman splittings were calculated by means of a "finite perturbation" technique. The external magnetic field B was varied between 0.0001 and 0.05 au, where 1 au corresponds to 1.715×10^3 T.[25,26] The velocity of light, c, is taken as 137.0360 au. Numerical values for the g-factors were then derived from

(21) Foster, J. M.; Boys, S. F. *Rev. Mod. Phys.* **1960**, *32*, 300.
(22) Wachters, A. J. H. *J. Chem. Phys.* **1970**, *52*, 1033.
(23) Huzinaga, S. *Approximate atomic functions. I and II. Preprints*; University of Alberta: Alberta, Canada, 1971.
(24) Hess, B. A.; Marian, C. M.; Wahlgren, U.; Gropen, O. *Chem. Phys. Lett.* **1996**, *251*, 365 and references therein.
(25) Whiffen, D. H. *Pure Appl. Chem.* **1978**, *50*, 75.

Table 1. Fine-Structure Splitting of the ^4F Ground State of the Free Co^{2+} Ion (in cm^{-1})

		$\xi = 1.0$			$\xi = 0.61$	$\xi = 0.582$
J	exptl[a]	^4F[b]	^4F, ^4P, ^2G[b]	full d^7	^4F[b]	full d^7
N_{SOC}[c]		28	58	120	28	120
$^9/_2$	0	0	0	0	0	0
$^7/_2$	841	1389	1469	1463	847	834
$^5/_2$	1451	2469	2576	2505	1506	1451
$^3/_2$	1867	3241	3348	3207	1977	1876

[a] References 2, and 15. [b] States which are included in the SOC-CI. [c] N_{SOC} is the dimension of the SOC-CI, see text.

the calculated energy splittings ΔE in given magnetic field B by means of eq 1, i.e., by using

$$g = -\frac{\Delta E}{\beta B \Delta M} \tag{10}$$

III. Mononuclear Co(II) Complexes

In order to adjust the parameter ξ and to analyze the effect of SOC on the electronic states of a single Co^{2+} ion, we first performed a series of calculations for the isolated Co^{2+} ion and for several mononuclear Co(II) complexes with octahedral or distorted octahedral geometries.

Table 1 contains our results for the fine-structure splitting of the ^4F ground state of the free Co^{2+} ion. In addition to diagonalizing the SOC Hamiltonian in the full space of all 120 states belonging to the d^7 configuration, we also limited the SOC-CI treatment to the 28 states which span the ^4F manifold and to the 58 states spanning ^4F, ^4P, and ^2G. An analysis of the errors introduced by such a truncation of the SOC-CI space was necessary since the full space could not be used in the corresponding calculations for the chlorine-bridged binuclear Co(II) complex (see section IV).

Table 1 shows that the ^4F ground state is split by SOC into four components with $J = {}^9/_2$, ${}^7/_2$, ${}^5/_2$, and ${}^3/_2$. The splitting depends to a certain extent on the subspace in which the SOC Hamiltonian is diagonalized, but this dependence is not very pronounced and does not show any systematic trend. The calculated energy differences are about 50% too large, as long as the unscaled one-electron spin−orbit Hamiltonian is employed, i.e., for $\xi = 1.0$. By using a scaling factor in the order of 0.6 the experimental fine-structure splittings[2,15] can be reproduced quite well. Of course, the precise value of this scaling factor will depend on the basis set and on the size of the space in which H_{SOC} is diagonalized. Table 1 shows that we can reproduce the experimental fine-structure splittings within about 10 cm^{-1} by using $\xi = 0.582$ when H_{SOC} is diagonalized in the full space of the d^7 configuration. In all subsequent calculations we will use $\xi = 0.61$, which is slightly better for the $J = {}^9/_2$ to $J = {}^7/_2$ splitting. This value for ξ will not be further readjusted for the mononuclear or binuclear complexes.

When the Co^{2+} ion is placed into an octahedral ligand field, the whole pattern of low-lying states is dramatically changed. In the present calculations we have considered five different situations:

(a) Co^{2+} in a pure point charge (PC) field which simulates the rock-salt structure of CoO. Point charges of ±2.0 and an interionic Co−O distance of 2.13 Å[27] have been used.

(b) A $[CoO_6]^{10-}$ cluster embedded in the same point charge field as before. In order to prevent the electrons at the six O^{2-} ions from flowing to the adjacent positive point charges, repulsive effective core potentials (ECPs) were added at all 18 cationic sites in the first coordination shells of the O^{2-} ions which are included explicitly in the cluster. As in our previous calculations for CoO[28,29] the semilocal electron-free pseudopotentials for Mg^{2+} published by Preuss et al.[30] were used for this purpose.

(c) An isolated octahedral $[CoCl_6]^{4-}$ complex, without further embedding. The Co−Cl bond length was chosen as 2.27 Å, which is in the range of the Co−Cl bond distances found by Couldwell and Husain[8] in mono- and binuclear Co complexes, but shorter than the corresponding distances in other chlorine-bridged cobalt compounds[8] and in Nühlen's $CoCl_3Co$ complex[11,12] (2.46 Å). In bulk $CoCl_2$, the Co−Cl distance is also substantially longer, namely, 2.51 Å.[27]

(d) A L_3CoCl_3 complex with the Cl^- anions placed along the positive and the model ligands L along the negative Cartesian axes (R(Co−Cl) = 2.46 Å, R(Co−L) = 1.683 Å). This complex represents one mononuclear moiety of the binuclear L_3CoCl_3-CoL_3 complex, but with ClCoCl angles of 90°. Of course, this complex has not the full O_h symmetry, but exhibits a small trigonal distortion to C_{3v} symmetry at the Co^{2+} ion.

(e) The same L_3CoCl_3 complex as before, but with the strong trigonal distortion of the ClCoCl angles as in the full binuclear complex ($\angle$ClCoCl = 85.66°). This complex has the same ligand field at the metal cation as the binuclear complex.

Tables 2 and 3 contain our results for the ligand-field and spin−orbit splittings of the ^4F ground state of Co^{2+} in the octahedral and distorted octahedral environments. The SOC Hamiltonian has been diagonalized in the full space of the 120 states of the d^7 manifold, in the reduced spaces with the dimensions 28 (^4F) and 58 (^4F, ^4P, ^2G), and also in the subspace of the 12 components of the $^4T_{1g}$ ground state of Co^{2+} in the ligand field with octahedral symmetry. The test calculations with $N_{SOC} = 12$ were necessary, since we used this subspace in the calculations for the binuclear complex (section IV). The results for $N_{SOC} = 28$ and 58 are so close to those for $N_{SOC} = 120$ that they are not included in the tables.

Table 2 shows that the octahedral ligand field splits the ^4F state of Co^{2+} into the $^4T_{1g}$ ground state, a first excited $^4T_{2g}$ state, and a second excited $^4A_{2g}$ state. The excitation energies are about 5500 and 12 000 cm^{-1}, for both CoO and $[CoCl_6]^{4-}$, but are considerably smaller for Co^{2+} in the PC field.[28] SOC splits the $^4T_{1g}$ ground state further into four components which belong to the irreducible representations $E_{1/2}$, $F_{3/2}$, $F_{3/2}$, and $E_{5/2}$ of the O_h* double group. (The Mulliken notation[31,32] for the spinor representations of the double groups will be used throughout the paper instead of the Bethe notation.[33] For O_h*, the representations $E_{1/2}$, $F_{3/2}$, and $E_{5/2}$ are identical to Γ_6, Γ_8, and Γ_7 in Bethe's notation.) As is well-known from text books on ligand field theory,[34] the second state of $F_{3/2}$ symmetry and the

(26) IUPAC *Quantities, Units and Symbols in Physical Chemistry*, 2nd ed.; Blackwell Scientific Publishers: Oxford, 1993.
(27) Wyckoff, R. W. G. *Crystal structures*, 2nd ed.; Interscience Publishers: New York, 196; Vol. 1, p 86.
(28) Shi, S.; Staemmler, V. *Phys. Rev. B* **1995**, *52*, 12345.
(29) Hassel, M.; Kuhlenbeck, H.; Freund, H.-J.; Shi, S.; Freitag, A.; Staemmler, V.; Lütkehoff, S.; Neumann, M. *Chem. Phys. Lett.* **1995**, *240*, 205.
(30) Preuss, H.; Stoll, H.; Wedig, U.; Krüger, Th. *Int. J. Quantum Chem.* **1981**, *19*, 113.
(31) Herzberg, G. *Molecular Spectra and Molecular Structure*; Van Nostrand: New York, 1967; Vol. 3.
(32) Altmann, S. L.; Herzig, P. *Point-group theory tables*; Oxford Science Publications, Clarendon Press: Oxford, 1994.
(33) Koster, G. F.; Dimmock, J. O.; Wheeler, R. G.; Statz, H. *Properties of the Thirty-Two Point Groups*; MIT Press: Cambridge, Massachusetts, 1963.

Table 2. Ligand-Field and Spin−Orbit[a] Splittings of the ^4F Ground State of Co^{2+} in Different Octahedral Environments (in cm^{-1})

		Co^{2+} + PC field			CoO			$[CoCl_6]^{4-}$		
		0[b,c]	12[b]	120[b]	0[b,c]	12[b]	120[b]	0[b,c]	12[b]	120[b]
$^4T_{1g}(12)$[d]	$E_{1/2}(2)$[e]	0	0	0	0	0	0	0	0	0
	$F_{3/2}(4)$		426	314		412	373		408	372
	$F_{3/2}(4)$		1135	856		1098	998		1087	987
	$E_{5/2}(2)$		1135	1139		1098	1112		1087	1101
$^4T_{2g}(12)$	$E_{1/2}(2)$	1935		2604	5428		6020	5659		6241
	$F_{3/2}(4)$			2676			6090			6306
	$F_{3/2}(4)$			2903			6186			6407
	$E_{5/2}(2)$			2994			6391			6611
$^4A_{2g}(4)$	$F_{3/2}(4)$	4406		5374	11942		12716	12489		13246

[a] $\xi = 0.61$. [b] N_{SOC}, dimension of the SOC-CI (see text). [c] Without SOC. [d] Without SOC, O_h symmetry group. The degeneracy of the states is given in parentheses. [e] With SOC, Mulliken notation[31,32] for the irreducible spinor representations of the O_h* double group. The degeneracy of the states is given in parentheses.

Table 3. Ligand-Field and Spin−Orbit[a] Splittings of the $^4T_{1g}$ Ground State of Co^{2+} in Trigonally Distorted L_3CoCl_3 Complexes (in cm^{-1})

state		∠ClCoCl = 90°			∠ClCoCl = 85.66°		
C_{3v}	C_{3v}*[b]	0[c,d]	12[c]	120[c]	0[c,d]	12[c]	120[c]
$^4E(8)$	$1E_{1/2}(2)$	0	0	0	0	0	0
	$2E_{1/2}(2)$	0	390	347	0	322	283
	$1E_{3/2}(2)$[e]	0	432	391	0	513	478
	$3E_{1/2}(2)$	0	1063	983	0	994	942
$^4A_2(4)$	$2E_{3/2}(2)$[e]	92	1106	1008	470	1238	1137
	$4E_{1/2}(2)$	92	1125	1092	470	1292	1268

[a] $\xi = 0.61$. [b] Mulliken notation.[31,32] [c] N_{SOC}, dimension of the SOC-CI (see text). [d] Without SOC. [e] The two one-dimensional spinor representations $^1E_{3/2}$ and $^2E_{3/2}$ (see refs 31 and 32) are combined into one line.

lowest state of $E_{5/2}$ symmetry remain degenerate as long as the SOC Hamiltonian is only diagonalized in the subspace of the 12 components of $^4T_{1g}$. This degeneracy is removed as soon as the dimension of the SOC-CI is enlarged to include also the $^4T_{2g}$ and $^4A_{2g}$ states (dimension 28). A further increase of the dimension of the SOC-CI up to the maximum of 120 leads to only small changes in the excitation energies. Since the spin−orbit coupling is mainly a property of the metal cation and not much influenced by the ligand field, the SOC splittings of the $^4T_{1g}$ ground states are very similar in the three cases presented in Table 2. The present excitation energies for CoO without SOC are nearly identical with our previous results[28,29] and those of de Graaf;[35] our results with SOC are also very similar to those of de Graaf though a much higher level of sophistication has been used for the calculation of the SOC effects in the latter study.[35]

As soon as the ligand field deviates from the ideal octahedral symmetry, the 12-fold degeneracy of the $^4T_{1g}$ ground state is removed by the geometrical distortion. Table 3 shows that there is a small splitting of 92 cm^{-1} into a lower ^4E and a higher $^4A_2$ state in the L_3CoCl_3 complex with all ligands along the Cartesian axes, even without SOC. The splitting is increased to 470 cm^{-1} in the strongly trigonally distorted L_3CoCl_3 complex and has about the same size as the SOC splittings in Table 2. If geometrical distortion and SOC splitting are combined, no degeneracies remain except for Kramers 2-fold degeneracy of a system with an odd number of electrons. The excitation energy of the first excited doublet is 283 cm^{-1} in the calculation with $N_{SOC} = 120$, but slightly larger, 322 cm^{-1}, for $N_{SOC} = 12$. Table 3 contains only the 12 low-lying states derived from the $^4T_{1g}$ ground state. As for the complexes with an undistorted octahedral environment in Table 2, the next states belonging to $^4T_{2g}$ and $^4A_{2g}$ follow at excitation energies of about 6500 and 13 000 cm^{-1} and are no longer considered in the following.

Table 4. *g*-Factors of the Components of the $^4T_{1g}$ Ground State of Co^{2+}

(a) In Octahedral Surroundings (O_h Symmetry)

		LFT[b]	Co^{2+} PC field		CoO		$[CoCl_6]^{4-}$	
state	J[a]	12[c]	12[c]	120[c]	12[c]	120[c]	12[c]	120[c]
$E_{1/2}$[d]	1/2	13/3	4.33	4.79	4.29	4.50	4.28	4.48
$F_{3/2}$	3/2	16/15	1.07	1.22[e]	1.02	1.07[e]	1.09	1.14[e]
$F_{3/2}$	5/2	3/5	0.61	1.21[e]	0.59	0.91[e]	0.63	0.92[e]
$E_{5/2}$				0.03[f]		0.16[f]		0.16[f]

(b) In Trigonally Distorted Octahedral Surroundings (C_{3v})

		∠L_3CoCl_3 = 90°				∠L_3CoCl_3 = 85.66°			
		$g_{\|\|}$		$g_\perp$		$g_{\|\|}$		$g_\perp$	
state	$\|M_J\|$[g]	12[c]	120[c]	12[c]	120[c]	12[c]	120[c]	12[c]	120[c]
$1E_{1/2}$[h]	1/2	4.59	4.79	4.14	4.33	6.37	6.60	3.10	3.24
$2E_{1/2}$	1/2	0.57	0.23	2.12	2.63	1.77	2.08	1.63	2.02
$3E_{3/2}$	3/2	0.93	1.08	0.00	0.00	0.31	0.40	0.00	0.00
$4E_{1/2}$	5/2	0.63	0.47	0.00	0.17	0.60	0.61	0.00	0.04
$5E_{3/2}$	3/2	0.79	0.99	0.00	0.00	1.36	1.68	0.00	0.00
$6E_{1/2}$	1/2	0.84	0.36	1.99	1.45	1.41	1.74	2.53	2.59

[a] Effective total angular momentum J. [b] Ligand-field theory.[34,36] [c] N_{SOC}. [d] O_h* double group, Mulliken notation.[31,32] [e] $J_{eff} = 3/2$; the outermost components for $M = 3/2$ and $M = -3/2$ are used to calculate g (see Figure 1). [f] Kramers doublet with $J_{eff} = 5/2$, i.e., $\Delta M = 5$ is used to calculate g from the splitting of the two components. [g] $\Delta M = 2|M_J|$ used to calculate g. [h] C_{3v}* double group; Mulliken notation.[31,32]

The comparison of the results for $[CoCl_6]^{4-}$ in Table 2 with those for L_3CoCl_3 (∠ClCoCl = 90°) in Table 3 shows that the use of He-like model ligands has no large effects. The replacement of three Cl^- ions with He-like ligands leads to a small splitting of the degenerate levels, but the separation of the energy levels remains essentially unchanged. Some additional calculations were performed for the distorted $[Cl_3CoCl_3]^{4-}$ complex; their results were very similar to those for the distorted L_3CoCl_3 complex. In particular the first $1E_{1/2} \rightarrow 2E_{1/2}$ energy difference amounts to 344 cm^{-1} in $[Cl_3CoCl_3]^{4-}$ instead of 322 cm^{-1} in L_3CoCl_3 (Table 3).

In Table 4 we have collected our results for the *g*-factors of the 12 low-lying states. As long as the ligand field has perfect octahedral symmetry, the **g**-tensor is isotropic (Table 4a). Our numerical results agree fairly well with the results of the early theoretical treatments.[34,36] If only the 12 components of the $^4T_{1g}$

(34) Griffith, J. S. *The theory of transition-metal ions;* Cambridge University Press: Cambridge, 1961.
(35) de Graaf, C. Ph.D. Thesis. Groningen, 1998.
(36) Abragam, A.; Pryce, M. H. L. *Proc. R. Soc. London* **1951**, *A 206*, 173.

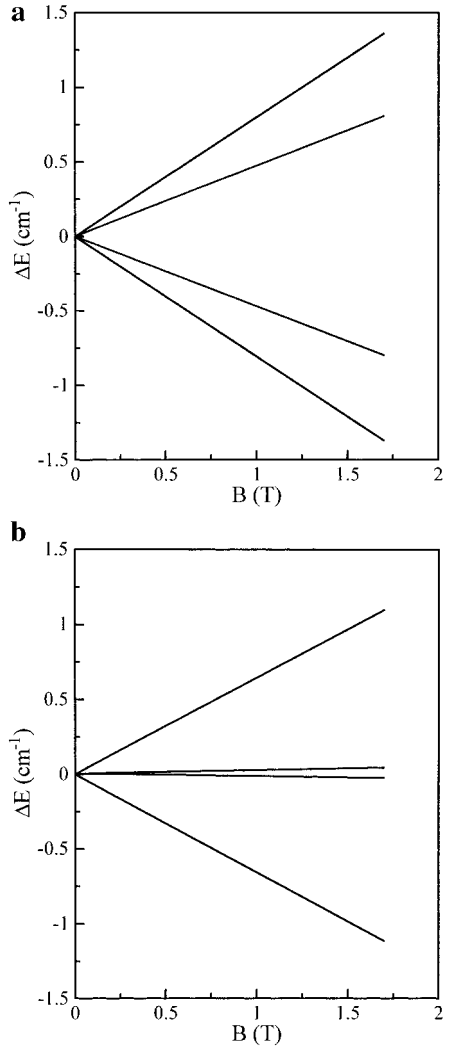

Figure 1. (a) Zeeman splitting of the lowest $F_{3/2}$ state of the $[CoCl_6]^{4-}$ complex. External magnetic field B in tesla. (b) Zeeman splitting of the second $F_{3/2}$ state of the $[CoCl_6]^{4-}$ complex. External magnetic field B in tesla.

ground state are included ("first order" Zeeman effect[34]) the g-factors which have been derived analytically for the weak field limit ($g = {}^{13}/_{3}$, ${}^{16}/_{15}$, and ${}^{3}/_{5}$ for $E_{1/2}$, $F_{3/2}$, and $F_{3/2} + E_{5/2}$[36]) are quite accurately reproduced. In this case, all components of $^4T_{1g}$ can be described by effective angular momentum quantum numbers J and M_J as indicated in Table 4a, and the Zeeman splitting is given by eq 1, i.e., all energy differences between states belonging to the same J and differing by $\Delta M_J = \pm 1$ are identical and amount to $g\beta B$.

The situation is more complicated for $N_{SOC} > 12$, i.e., if the interaction with the higher states of the d^7 manifold is included. The g-factor of the $E_{1/2}$ ground state is not much affected; it is only slightly enhanced to 4.79 (Co^{2+} in the pure PC field) or 4.50 (CoO and $[CoCl_6]^{4-}$). However, the Zeeman splitting of the two $F_{3/2}$ states can no longer be described by a single g-factor. Figure 1 shows that the splitting is linear in B and symmetric with respect to $B = 0$, but not proportional to M. Finally, the splitting of the highest Kramers doublet, $E_{5/2}$, is very small. In semiempirical calculations using the angular overlap model a similar behavior has been found.[37]

The trigonal distortion leads to substantial changes in the components of the **g**-tensors, in particular to large anisotropies.

(37) Schönherr, T. Private communication.

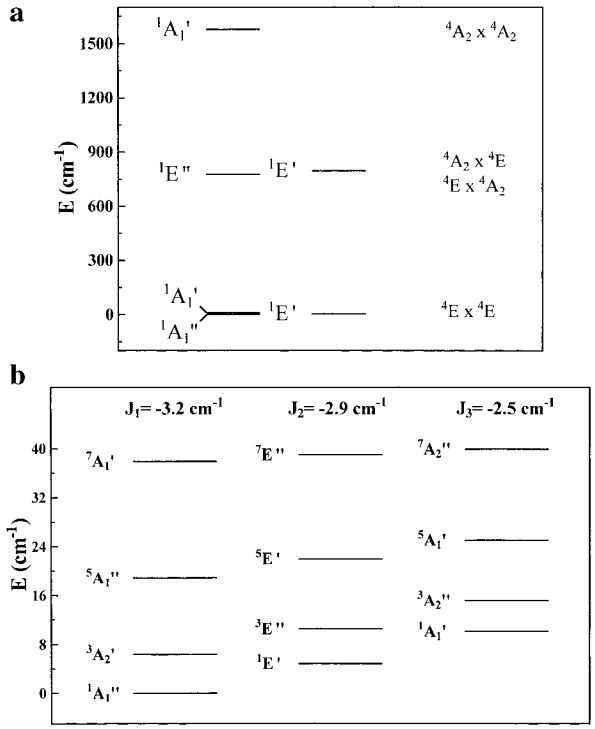

Figure 2. Energy levels of the low-lying electronic states of the $L_3CoCl_3CoL_3$ complex, without spin−orbit coupling. (a) All low-lying singlet states. (b) All spin states belonging to the $^4E \times {}^4E$ manifold in an extended scale.

This is shown in Table 4b, which contains the principal values, $g_{||}$ and $g_{\perp}$, for the two distorted complexes. For those Kramers doublets which belong to the 2-fold-degenerate spinor representation $E_{1/2}$ of the C_{3v}* double group,[32] $g_{||}$ and $g_{\perp}$ are both different from zero. For the doublets belonging to the two components of $E_{3/2}$, $g_{\perp}$ has to vanish. Table 4b shows that even for the small trigonal distortion the deviations from the isotropic values as given in Table 4a are quite large, while the extension of N_{SOC} from 12 to 120 does not lead to dramatic changes.

The g-factors of the lowest Kramers doublet of Co^{2+} ions in trigonally distorted octahedral ligand fields have been first treated analytically by Abragam and Pryce.[36] Using crystal-field theory and reasonable empirical values for the parameters involved, these authors obtain $g_{||} \approx 6$ and $g_{\perp} \approx 3$, which is in good agreement with the experimental values observed for several complexes.[34,36] Table 4b shows that our numerical results for the strongly distorted L_3CoCl_3 complex are consistent with both semiempirical theory and experiment. To the best of our knowledge, the g-factors of the higher Kramers doublets of Co^{2+} have been neither measured nor treated analytically so far.

IV. Binuclear $L_3CoCl_3CoL_3$ Complex. The number of low-lying electronic "pair" states of the binuclear chlorine-bridged $L_3CoCl_3CoL_3$ complex is quite large. As long as both trigonal distortion and SOC are neglected, the 12-fold degeneracies of the $^4T_{1g}$ ground states of the two Co^{2+} cations will give rise to $12 \times 12 = 144$ closely spaced states,[13] nine singlets, triplets, quintets, and septets, which are only split by the rather weak superexchange interaction through the three Cl bridges. Inclusion of trigonal distortion and SOC will strongly modify the whole pattern of low-lying electronic pair states.

Figure 2a contains an energy level diagram for the nine singlet "pair" states of the binuclear complex, calculated without inclusion of SOC. Because of the splitting of the $^4T_{1g}$ ground state at either Co^{2+} ion into a lower ^4E and a higher $^4A_2$ component, the $L_3CoCl_3CoL_3$ complex has four low-lying

Table 5. Low-Lying Electronic States of $L_3CoCl_3CoL_3$ (SOC Included)

manifold[a]	pair state[b]	ΔE, cm^{-1}	ΔE,[c] cm^{-1}	ΔE_{extr},[d] cm^{-1}
$1E_{1/2} \times 1E_{1/2}$	A_2''	0.0	16.4	0.0
	A_1'	4.6	10.5	15.0
	E''	20.2	0.0	57.0
$1E_{1/2} \times 2E_{1/2}$	E'	308.4	308.0	
	A_1''	309.7	299.1	
	A_2''	310.8	307.4	
	E''	315.3	310.6	
	A_2'	315.4	311.1	
	A_1'	325.6	313.4	
$1E_{1/2} \times 1E_{3/2}$	E'	547.7	542.2	
	E''	548.5	544.4	
	E''	550.6	550.8	
	E'	555.9	551.1	
$2E_{1/2} \times 2E_{1/2}$	A_2''	611.8	608.2	
	E''	617.5	611.5	
	A_1'	618.9	612.6	

[a] States of the mononuclear L_3CoCl_3 complexes (including SOC), compare Table 3. [b] Irreducible representation of D_{3h}*. [c] "Ferromagnetic" coupling case: Only the covalent configurations are included in the valence SOC-CI. For details, see text. [d] Extrapolated, see text.

singlet states, derived from $^4E \times {}^4E$, and the next singlets follow at about 700 cm^{-1} ($^4E \times {}^4A_2$ and $^4A_2 \times {}^4E$) and 1500 cm^{-1} ($^4A_2 \times {}^4A_2$). The superexchange interaction between the two Co^{2+} ions is very weak, with exchange integrals J of about -3.0 cm^{-1}. Therefore the exchange splitting would be hardly visible in the scale of Figure 2a. Each of the lines in the figure represents a whole Landé pattern with one singlet, one triplet, one quintet, and one septet state, with relative energies of about 0.0, 6.0, 18.0, and 36.0 cm^{-1}. Since J is negative, the singlets are the lowest components of each Landé ladder. Figure 2b contains all levels belonging to the $^4E \times {}^4E$ manifold in an extended scale.

As in the mononuclear complexes, the whole pattern of low-lying states is completely changed as soon as SOC is included. If the ground state Kramers doublets (Table 3) at the two Co^{2+} ions are coupled, four pair states will evolve which belong to the representations A_1', A_2'', and E'' of the D_{3h}* double group and which are separated by the superexchange interaction. The next eight states are expected at about 300 cm^{-1} (ground state doublet of one Co^{2+} ion coupled to the first excited doublet of the other Co^{2+} ion and vice versa).

Table 5 contains the numerical results of our SOC-CI calculation for all states of $L_3CoCl_3CoL_3$ below 800 cm^{-1}. The two lowest states are nondegenerate; they have A_2'' and A_1' symmetry and are separated by 4.6 cm^{-1}. The next state is 2-fold degenerate (E'') and 20.2 cm^{-1} higher than the A_2'' ground state. This pattern of two singlet and one doublet pair states cannot be described by the phenomenological Heisenberg Hamiltonian as given in eq 3, which would couple two doublets ($S = {}^1/_2$) to one singlet ($S = 0$) and one triplet, separated by $2J$. In the present case, two independent energy differences are needed for describing the energy spacings between the four lowest exchange-coupled pair states. (One should be careful calling the two lowest states "singlet" states, though they are not degenerate. But the term "singlet" has lost its conventional meaning for the spin quantum number $S = 0$ in a system where SOC strongly mixes states with different spin multiplicities.) The sequence of states found in the present calculations is rather similar to the one in $Ti_2Cl_9^{3-}$ which has been discussed—with the inclusion of SOC terms—in ref 1.

The next set of excited levels is closely spaced at about 300 cm^{-1} and consists of the eight states which are obtained by coupling the ground state doublet of one Co^{2+} ion ($1E_{1/2}$) with the excited doublet ($2E_{1/2}$) of the other one. All higher excited pair states can be derived as well by combining the levels at the two metal centers.

The dimension of the full SOC-CI matrix is quite large. Since the superexchange interaction is caused by charge transfer excitations from one Co^{2+} ion to the neighboring one, the full active space of 10 3d-orbitals occupied by 14 electrons has to be used. Furthermore, all values of M_S have to be included as well. This gives a total of 38 760 configurations. As we have pointed out before, we have evaluated the matrix elements of the SOC and Zeeman Hamiltonians only in the subspace of the 12×12 states spanned by the eigenvectors of the nonrelativistic VCI for the two Co^{2+} cations in their $^4T_{1g}$ ground states. This limitation has no influence on the splitting between the four lowest states; however, as is obvious from Table 3, the states at about 300 cm^{-1} would be probably lowered by $\sim$40 cm^{-1} if the full space were used instead.

As is well-known, the superexchange interaction is largely underestimated at the level of VCI or CASSCF calculations. The main reason is that the energies of the charge transfer configurations (i.e., the $d^{n-1}d^{n+1}$ excitations) are much too high as long as they are calculated from orbitals which have been optimized for the neutral d^nd^n configurations and no electronic relaxation is taken into account. Since we cannot, for the time being, combine MCCEPA[20] calculations which account for dynamical correlation and relaxation effects with the present SOC-CI, we have estimated the influence of the relaxation effects in the following way:[6,7] In addition to the full VCI, we have performed a truncated VCI in which only the covalent configurations (i.e., the d^nd^n configurations) are included. In this way, the superexchange coupling is excluded and only the direct exchange survives. Of course, this decoupling of direct exchange from superexchange is meaningful only if the active orbitals are localized.[6,7] The results of this truncated VCI are also included in Table 5. Now, the E'' state is the lowest state, and A_1' and A_2'' follow at 10.5 and 16.4 cm^{-1}. That means that the "high-spin" E'' state is the ground state and the coupling is ferromagnetic if only the direct exchange is accounted for. The superexchange mechanism lowers the A_2'' state by 36.6 cm^{-1} (from $+16.4$ to -20.2 cm^{-1} relative to E'') and the A_1' state by 26.1 cm^{-1} (from $+10.5$ to -15.6 cm^{-1}, again relative to E''). Generally, the superexchange contribution to J is underestimated in the VCI calculation by a factor of about 2.0.[6,7] Therefore, one can obtain a realistic estimate of the relative energies of the lowest spin states by fixing the direct magnetic exchange at its VCI value and multiplying the superexchange contribution by a factor of 2; i.e.,

$$J = J_{DE} + \alpha J_{SE} \quad \text{with} \quad \alpha = 2.0 \tag{11}$$

In this way we find that the A_2'' "singlet" state remains the ground state, and the next "singlet", A_1', is moved slightly upward to about 15 cm^{-1}, while the E'' doublet state is shifted substantially to an energy of about 57 cm^{-1} (Table 5).

The behavior of the four low-lying states in an external magnetic field parallel and perpendicular to the C_3 axis of the $L_3CoCl_3CoL_3$ complex is shown in Figure 3. If the field is parallel to the C_3 axis, the degeneracy of the two components of E'' is removed. The Zeeman splitting is linear in $B_\parallel$ and corresponds to $g_\parallel = 14.06$, which is about twice as large as $g_\parallel$ for the trigonally distorted mononuclear complex. Figure 3 shows that the two singlet states, A_2'' and A_1', exhibit only small Zeeman shifts which are quadratic in $B_\parallel$ (second-order Zeeman effect). An external field $B_\perp$ perpendicular to the C_3 axis does

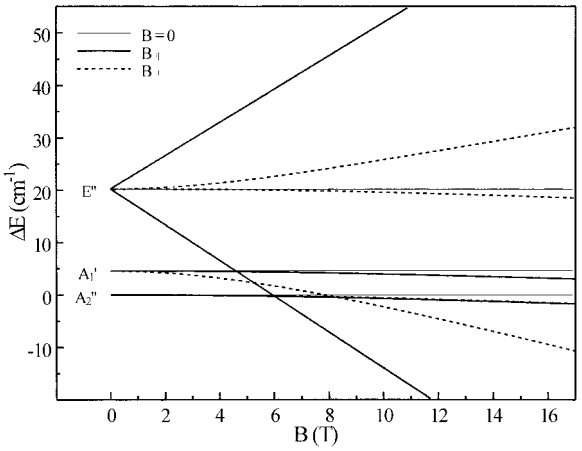

Figure 3. Zeeman splitting of the four low-lying electronic states of the $L_3CoCl_3CoL_3$ complex in an external magnetic field: full lines, $B_{||}$; dashed lines, $B_{\perp}$; thin lines, $B = 0$. For the A_2'' ground state the behavior in $B_{\perp}$ is identical to that in $B_{||}$.

not lead to a splitting of E″. It causes, however, an interaction between A_1' and one component of E″, since the Zeeman Hamiltonian has a nonzero off-diagonal matrix element between the respective wave functions. As long as this matrix element is small compared to the energy difference $E(E'') - E(A_1')$, the effect is quadratic in $B_{\perp}$, but becomes linear for larger fields. The A_2'' state and the other component of E″ show again small shifts which are quadratic in $B_{\perp}$. For small perpendicular fields, $B_{\perp} < 0.1$ T, the magnetic behavior of all four states can be described by $g_{\perp} = 0$; however, the second-order effects are already visible in the susceptibilities at $B_{\perp} = 1$ T.

Using the calculated energy levels of the low-lying spin states, with and without an external magnetic field, we can directly evaluate the magnetic susceptibility $\chi(T)$ by a Boltzmann average over all accessible states. Since we have used a finite-field approach for the magnetic field, we replace the differentiation with respect to B by finite differences and obtain

$$\chi_\alpha(T) = \frac{M_\alpha}{B} = -\frac{N_A}{B^2}\{\sum_n (E_n(B_\alpha) - E_n(0)) \exp(-E_n(B_\alpha)/kT)\}\{\sum_n \exp(-E_n(B_\alpha)/kT))\}^{-1} \quad \text{with} \quad \alpha = ||, \perp \quad (12)$$

where N_A is Avogadro's number and M_α are the components of the macroscopic molar magnetization.[1]

In Figure 4 we have plotted the calculated parallel and perpendicular components of χ for temperatures up to 100 K. In this temperature range only the four lowest spin states of the complex are populated. The calculations were performed for a magnetic field strength of 1 T, which is the field strength used in the experimental study.[12] The figure documents the strong magnetic anisostropy of the complex, which has a large parallel component $\chi_{||}$ while $\chi_{\perp}$ is comparatively small for all temperatures. Both components show a typical antiferromagnetic behavior, with small values in the vicinity of $T = 0$, broad maxima at intermediate temperatures (20−50 K), and a slow decay which behaves approximately like $1/T$ at high temperatures.

Figure 4 shows very clearly that the form of the susceptibility curves depends very sensitively on the spacing between the electronic energy levels. The pronounced maximum of $\chi_{||}$ at 20 K, obtained with the original ab initio energy levels, is

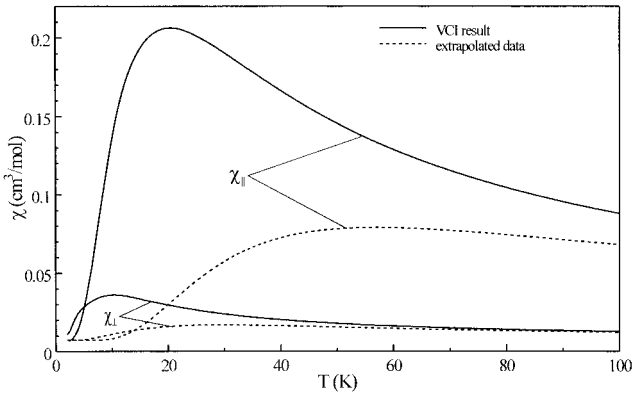

Figure 4. Parallel and perpendicular components of the magnetic susceptibility of $L_3CoCl_3CoL_3$ as a function of temperature. Full lines: Calculation with the original ab initio excitation energies of 4.6 and 20.2 cm^{-1}. Dashed lines: Extrapolated excitation energies of 15 and 57 cm^{-1}, respectively (see text).

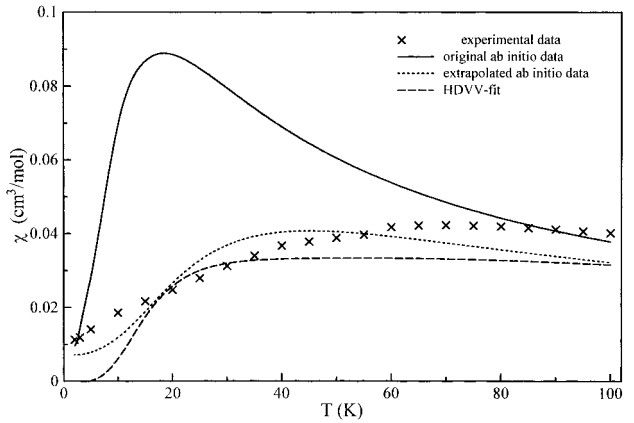

Figure 5. Comparison between calculated and experimental magnetic susceptibilities of $L_3CoCl_3CoL_3$: (×) experimental data; (—) original ab initio excitation energies; (---) extrapolated excitation energies, 15 and 57 cm^{-1}; (— — —) HDVV fit from ref 12.

considerably lowered and shifted to higher temperatures when the extrapolated energy levels of 15 and 57 cm^{-1}, respectively, are used (Table 5, column 5). (The calculated Zeeman splittings were kept unchanged.) This effect is also typical for antiferromagnetic systems. The larger J, the higher temperatures are required to markedly populate the excited high-spin state the degeneracy of which is removed by the external magnetic field.

The behavior of $\chi_{\perp}$ is less sensitive to the spacing of the electronic levels. $\chi_{\perp}$ is different from zero only at temperatures which allow a population of the first excited A_1' state which is stabilized by the magnetic field through the interaction with one component of E″. This effect is markedly smaller than the first-order Zeeman effect responsible for $\chi_{||}$ and decays less rapidly with increasing temperature.

Figure 5 contains a comparison of the present results with the experimental data of Wieghardt and co-workers.[11,12] Since the tensor components of $\chi(T)$ have not been measured separately, Figure 5 contains our results also in form of the average susceptibility

$$\chi(T) = {}^1/_3(2\chi_{\perp} + \chi_{||}) \quad (13)$$

The experimental data are included in two different ways, (a) by plotting the raw data of Nühlen[11] and (b) using the fit with an isotropic HDVV (Heisenberg−Dirac−van Vleck) operator of the form

$$H = -2J\vec{S}_1\cdot\vec{S}_2 + \sum_{i=1}^{2}\left\{D_i\left(S_{zi}^{\,2} - \frac{S_i(S_i+1)}{3}\right) + \beta g_i\vec{S}_i\cdot\vec{B}_i\right\} \quad (14)$$

which contains three adjustable parameters: g, J, and D.[12] The spin quantum numbers S_1 and S_2 are chosen as $^3/_2$, i.e., as the original spin quantum numbers of the Co^{2+} ions in their ^4F ground states. The isotropic g-factors g_i and zero-field splitting parameters D_i are of course identical for the two ions.

With the values $J = -13.1$ cm^{-1}, $g = 2.86$, and $D = +40$ cm^{-1} as published by Bossek et al.[12] one obtains an excellent fit for $\chi(T)$ at temperatures above 100 K (this is not shown in Figure 5). In the low-temperature regime, the quality of the fit is much worse. By changing the sign of D, one gets less good agreement for $T > 100$ K, but a reasonable fit for low temperatures (Figure 5). However, there are still substantial deviations between the fit and the experimental data, in particular for $T < 40$ K. Figure 5 shows that our original ab initio results for $\chi(T)$ do not even qualitatively reproduce the experiment. The large maximum at about 20 K is clearly an artifact of the calculations. However, $\chi(T)$ calculated from the extrapolated excitation energies of 15 and 57 cm^{-1}, respectively, yields reasonable agreement with the measured values for $\chi(T)$. The deviations are of the same order as those obtained by fitting the parameters in the HDVV operator to the experimental data, despite the fact that our $\chi(T)$ does not contain any adjustable parameter.

We have only plotted $\chi(T)$ for temperatures below 100 K. For $T > 100$ K all curves decay smoothly and monotonically and behave similarly as in the interval between 75 and 100 K; however, the decay of the ab initio curves is slightly too rapid.

The experimental data for $\chi(T)$ seem to reach a finite nonzero value at $T = 0$.[11,12] The authors state that this is not caused by a monomeric paramagnetic impurity. The HDVV operator (eq 14) does not contain terms which can generate a nonzero contribution for $\chi(T)$ at very low T; therefore the HDVV fit goes to zero for $T < 3$ K. In our ab initio calculations, on the other hand, $\chi(T)$ remains nonzero even for $T = 0$, with a value of 0.0071 cm^3 mol^{-1}, which is not too far from experiment with a value of 0.0113 cm^3 mol^{-1} at 2 K.[11] The detailed analysis shows that this finite value is caused by the second-order Zeeman effect, which slightly lowers the A_2'' ground state for nonzero magnetic fields. This stabilization of A_2'' gives rise to a small contribution to χ, which is the only contribution at very low temperatures, when the low-lying first excited A_1' state is thermally not yet markedly populated. This contribution is isotropic since the stabilization of A_2'' is independent of the direction of the external magnetic field. We have to admit that the second-order Zeeman effect is very small, about 0.006 cm^{-1} at $B = 1$ T, i.e., at the limit of the numerical significance of our results. However, by increasing the magnetic field strength we were able to verify that the energy lowering of the A_2'' ground state is indeed quadratic in B.

So far we did not adjust our results (energy spacings, first- and second-order Zeeman splittings) to the experimental data, except for extrapolating the superexchange contribution to the exchange coupling by introducing the factor $\alpha = 2$ in eq 11. One can get a slightly better agreement with the experimental data by choosing $\alpha \approx 1.8$, which corresponds to excitation energies of 13 and 50 cm^{-1}, respectively, instead of 15 and 57 cm^{-1} (Table 5). If we adjust the two excitation energies independently, we obtain $\Delta E_1 = 3$ cm^{-1} and $\Delta E_2 = 48$ cm^{-1}. The temperature dependence of $\chi(T)$ is indeed rather insensitive to changes in ΔE_1, which means that ΔE_1 can be hardly determined experimentally from susceptibility data. (Obviously, $\chi_{\parallel}(T)$ does not depend at all on ΔE_1 since the first excited A_1' state experiences only a second-order Zeemann shift as does the A_2'' ground state; $\chi_{\perp}(T)$ depends weakly on ΔE_1 because of the coupling between A_1' and E''.) The good agreement between our extrapolated value for ΔE_2 (57 cm^{-1}) and the best fit (48 cm^{-1}) supports our confidence in the modified VCI results.

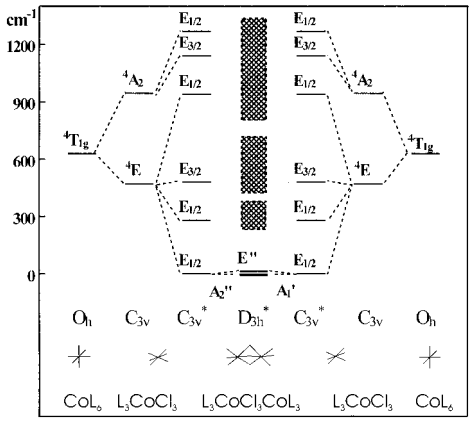

Figure 6. Splitting of the $^4T_{1g}$ ground states of Co(II), by trigonal distortion, spin−orbit coupling, and exchange interaction.

We have also fitted all relevant parameters (ΔE_1, ΔE_2, first- and second-order Zeeman splittings) to the experimental susceptibility data in the low-temperature regime. This resulted in a perfect reproduction of the experimental curve; however, the parameters obtained in that way were not very meaningful. The main problems connected with such a fit are as follows: (a) Are the susceptibilities so independent of the terminal ligands that the complex with our model ligands can be compared in all details with complexes possessing real ligands? (b) Can it be really excluded that the experimentally observed low-temperature behavior is not influenced by a paramagnetic impurity? (c) Are the theoretical results numerically so stable that one can rely on very small energy differences? Therefore, we are convinced that the calculated g-factors together with the extrapolated energy differences of 15 and 57 cm^{-1} yield a more realistic description of the low-lying states of the $L_3CoCl_3CoL_3$ complex than a perfect fit to the experimental susceptibility data.

V. Conclusions

Our main results for the energy levels of the low-lying electronic states of the $L_3CoCl_3CoL_3$ complex are summarized in Figure 6. The $^4T_{1g}$ ground states of the two Co^{2+} cations, which are 12-fold degenerate in perfect octahedral ligand fields (O_h symmetry) as long as spin−orbit coupling is neglected, are split by the local trigonal distortion (C_{3v} symmetry) and by spin−orbit coupling. Both effects are of the same order of magnitude, 200−500 cm^{-1}. Their combined action generates for each of the two Co^{2+} cations a 2-fold-degenerate ground state, belonging to the two-dimensional spinor representation $E_{1/2}$ of the double group C_{3v}*. All other states are at least 300 cm^{-1} higher in energy. The exchange coupling between the two $E_{1/2}$ ground states gives rise to four low-lying pair states for the complex: a A_2'' ground state, a first excited A_1' state, and a 2-fold-degenerate second excited E'' state. The excitation energies are calculated to be about 15 (A_1') and 57 cm^{-1} (E''), respectively. A bunch of eight excited states follows at about 300 cm^{-1}; the rest of the 144 low-lying pair states is rather closely spaced between 500 and 1500 cm^{-1}. In Figure 6 these manifolds of states are indicated by hatched areas.

The exchange coupling in $L_3CoCl_3CoL_3$ is "antiferromagnetic" in the sense that the lowest pair state is nondegenerate ("singlet") and is not affected in first order by an external magnetic field. Only the second excited state is degenerate and shows a Zeeman splitting in a magnetic field parallel to the molecular axis.

The experimentally observed temperature dependence of the magnetic susceptibility $\chi(T)$ of the $CoCl_3Co$ complex has been analyzed in terms of a phenomenological HDVV spin-Hamiltonian.[12] Though a reasonable fit to the experimental data could be obtained, the underlying model is definitely wrong. The comparison of Figure 2a,b and Figure 6, containing the energy levels of the pair states without and with spin−orbit coupling, respectively, shows that spin−orbit coupling drastically changes the whole pattern of low-lying states.

The calculated magnetic susceptibility possesses a large anisotropy, $\chi_{\parallel}$ being much larger than $\chi_{\perp}$ at all temperatures higher than about 10 K. The reason is that the second excited state, E″, experiences a linear Zeeman splitting only if the external magnetic field is oriented along the molecular axis. In a perpendicular field, only a second-order Zeeman effect is present, which is due to a coupling between the first excited A_1' state and one component of E″. At laboratory fields ($\sim$ 1 T) the second-order Zeeman effect is smaller than the first-order effect, which is the reason that $\chi_{\perp}$ is smaller than $\chi_{\parallel}$.

The experimental susceptibility data can be well reproduced by the ab initio calculations. $\chi(T)$ is very sensitive to the energy difference between the A_2'' ground state and the E″ excited state, but does not depend markedly on the difference between A_2'' and the first excited state A_1'.

Acknowledgment. The authors thank Prof. K. Wieghardt and Dr. D. Nühlen (Max-Planck-Institut für Strahlenchemie, Mülheim) for many discussions on the subject of this paper. Financial support by Deutsche Forschungsgemeinschaft, Ministerium für Wissenschaft und Forschung des Landes Nordrhein-Westfalen, and Fonds der Chemischen Industrie is gratefully acknowledged. K.F. is member of the Graduiertenkolleg "Dynamische Prozesse an Festkörperoberflächen", sponsored by the Deutsche Forschungsgemeinschaft. C.W. benefited from a grant of the Max-Buchner-Forschungsstiftung.

IC990280N